SAE International™

Metal-Oxide Particles in Combustion Engine Exhaust

2010-01-0792
Published
04/12/2010

Andreas C. Mayer
TTM, Technik Thermische Maschinen, CH

Andrea Ulrich
EMPA, Federal Labs, Dübendorf, CH

Jan Czerwinski
AFHB, Univ. of Appl. Sciences, Biel, CH

John J. Mooney
LLC, USA

ABSTRACT

Concern for engine particle emission led to EC-regulations of the number of solid particles emitted by LDV and HDV. However, all conventional piston-driven combustion engines emit metal oxide particles of which only little is known. The main sources are abrasion between piston-ring and cylinder, abrasion of bearing, cams and valves, catalyst coatings, metal-organic lubrication oil additives, and fuel additives. While abrasion usually generates particles in the µm-range, high concentrations of nanosize metal oxide particles are also observed, probably resulting from nucleation processes during combustion. In general, metal oxides, especially from transition metals, have high surface reactivity and can therefore be very toxic, especially nanosize particles, which evidently provide a high specific bioactive surface and are suspected to penetrate into the organism. Hence, these particles must be scrutinized for quantity, size distribution and composition.

Published data are summarized and data from investigations of various engines with respect to metal oxide particle emission are reported. These investigations were performed without and with VERT approved particle filters, where VERT is an international verification standard for emission reduction technologies, which, besides of filtration effectiveness, durability and limited pollutants also includes the analysis of secondary emissions, potentially formed by these technologies and of size specific metal emissions.

In good agreement with literature, the overall metal mass in the exhaust of IC-engines without particle filter is in the range of 0.1-1 mg/km metal. This combines wear metals and metals from lubrication oil additives. Size specific chemical analysis has shown that a large part of metal oxide particles are to be found in the size classes below 60 nm. However there are more metal oxide particles in the exhaust attached to soot particles of larger size, as chemical analysis also revealed. If there are less soot particles prevalent, like at idle conditions some of them do appear unattached in a separate fraction of much smaller size. SMPS particle size distribution at idle shows peaks of up to 10^8 particles per cc in the size range of 10-30 nm. It must be assumed that these are all metal oxide particles since PMP sampling was applied which means that these particles survived 300 °C and thus can not be volatiles.This high number of solid metal oxide particles implies a potential health risk. Hence, there is a need to further focus on small metal oxide particle emissions. For Diesel engines, industry has demonstrated that particle filters are available which can very efficiently filter those nanoparticles. There is little known about metal oxide emissions of other engines but it must be anticipated that all IC piston engines do emit such particles. Elimination of such metal oxide particles by highly efficient filtration therefore

might become an urgent future requirement for all engine categories.

INTRODUCTION

Assuming a linear dose/effect relationship, the defining toxicity parameter is the product of specific toxicity and dosage. The biological impact depends on the particles' ability to defeat the human body defense. Crucial factors are particle size, chemical composition and solubility. Insoluble particles are hazardous especially in small size ranges [1]2]. Toxicological studies have shown increased toxicity of nanoparticles compared to micrometer particles of the same composition, which has raised concern about the impact on human health [3]. Black carbon particles (soot) and many metal oxide particles are practically not soluble and appear in the nm-fraction of the exhaust gas of spark ignited and compression ignition engines.

The significance of particle size can be estimated from the alveolar deposition. See Fig. 1 and [6]. This relationship is valid for particle mass as well as for number and surface.

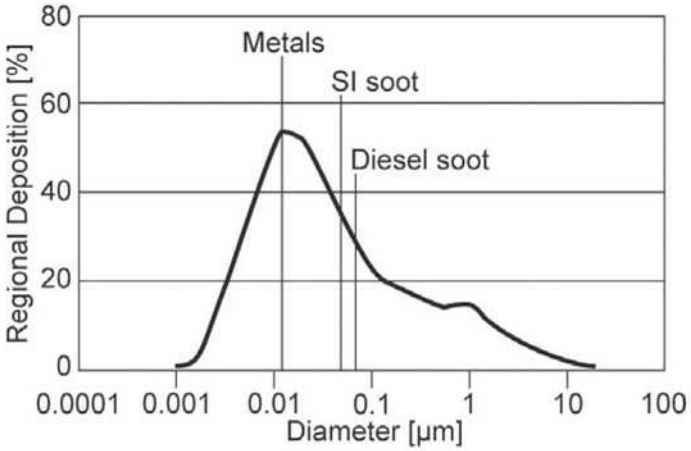

Fig. 1. Size specific deposition of nose-inhaled particles in the human alveoli [9]. Diesel soot particles (mean diameter 80 nm = 0.08 µm), SI soot particles (50 nm) and free metal oxide particles (15 nm) are all in the range of maximum alveoli deposition.

Figure 1 shows that particles < 10 µm can intrude deep into the lungs. Below 200 nm deposition in the alveoli is increasing with decreasing particle diameter to about 10 nm. Particles smaller than 10 nm are so mobile that many of them are already deposited in the upper airways. High concentrations of solid particles in the alveoli can overload the lung's defense mechanisms, which in the alveoli is only clearance by macrophage cells.

These small metal-oxide particles, discussed here, can penetrate the alveoli tissue and enter into the blood circulation [7]. Subsequently, these nanoparticles might be rapidly transported into the entire organism. Similar to the soot particles, the metal-oxide particles can cross the blood brain barrier and can also cross the placenta and enter into the fetus. The nanoparticles also can enter the brain via the olfactory nerve ending in the nose. The biological impact of nanosize particles is being intensively researched [3,4,5,6,7]; medical research is also focusing on cell toxicity due to metal and metal oxide particles [52,53,54,55]

The major known toxic effects are as follows.

• Smaller particles are more cytotoxic than larger particles [3,76].

• Particles < 200 nm can penetrate cell membranes [52,53]

• Particles can cause oxidative stress that is the precursor to inflammation [3].

• Iron, Copper, Vanadium and Zinc particles [5] and generally all transition metals, are considered to be critical for humal health. This is because of their high surface activity [15], which is indeed used in emission control catalysts.

Moreover, these extremely fine and insoluble particles can transport other surface adhered toxic substances, a phenomenon that is described as the “Trojan horse” effect [16]. This applies to all airborne particles but the effect becomes stronger with the high specific surface of engine exhaust solid particles.

Consequent to the above evidence, and ongoing investigations, responsible institutions recommend restricting body intruding insoluble metal emissions to an extreme minimum [17]. Oxide particles of Iron, Copper and Zinc, which are typical for emissions from combustion engines, may be 10 - 100 times more toxic than soot particles [18].

This paper does not intend a to provide a systematic comparison of the rapidly increasing number of biological studies but to demonstrate that there is sufficient evidence of a very high health risk due to metal oxide particles in engine exhaust which should motivate engineers to develop measures to prevent damage.

METAL OXIDE PARTICLE EMISSIONS DUE TO ABRASION

Material is abraded from piston ring and cylinder liner, from valve cams and valves, and from the bearings. These phenomena occur in all piston engines, and cannot be prevented, probably even not in future engine designs. Mainly the metals Fe, Cr, Ni are abraded due to friction between the piston-ring and cylinder-liner. Cu and Pb originate from the bearings. The piston-cylinder wear is very well investigted. The publications of Hannoschöck [26] and Eberle [27] describe the processes in detail. Abrasion is not

much dependent on the piston velocity. The bigger factor is the number of stroke reversals, i.e. RPM dependent. This explains why SI engines, which usually run at higher RPM, abrade almost twice as much metal as Diesel engines. This also explains to some extent the higher durability of Diesel engines.

The mass of abraded metal is about 0.1 to 1 mg/km [29]. It consists mostly of Iron as well as some Aluminum and Copper. Excessive abrasion occurs during lubrication deficit, i.e. especially at cold start. Above average abrasion is prevalent during short trips, e.g. urban stop-and-go driving. Therefore it can be assumed that metal oxide emission is highest under urban driving conditions.

Comprehensive data is available for different engine types [31]; Heavy-duty vehicle tests compared Diesel engines (with and without particle filter) against CNG fueled SI engines. The Diesel engines, without particle filter, emitted about 0.5 mg/km of abraded metals such as Fe and Cu. Several CNG SI engines emitted twice as much. The CARB investigation [32] reports total metal-oxide emissions from 0.5 to 1.5 mg/km from HDV in various driving cycles.

The abrasion process normally produces particles in the low µm range, the smallest maybe 1-2 µm. They will probably be washed away by the oil film and may end up in the lubrication oil sump or oil filter unless they participate again in the combustion process. Israel [30], when finding high concentration of nanosize particles in ambient air close to roads developed the hypothesis that these particles being re-entrained into combustion can be vaporized and re-condensed forming particles in the nm-range.

METAL OXIDE PARTICLE EMISSIONS FROM OIL AND FUEL ADDITIVES

Most industrialized nations legislate limits for the Pb and Mn content of fuels for road traffic. However, many countries do not curb fuel additives for off-road engines. Also uncontrolled are light and medium heating oils, and heavy oils fueling ships. Interestingly, nowhere is the metal content of vehicular lubrication oils regulated. Metallic additives in lubrication oils have important functions, e.g. decrease friction, inhibit corrosion, clean deposits and constrain sulfur-induced acidification. Mostly Zn and Ca compounds are used in metal-organic form. The average metal content of fresh commercially available lubrication oils is:

Zinc:	0.1 - 0.2 %
Calcium:	0.5 %
Boron:	0.09 %
Magnesium:	0.002-0.004 %

After prolonged deployment, the lubrication oil usually also contains abraded Iron, Copper, Lead, Aluminum and Nickel, which also can be re-entrained into the combustion chamber and be exposed to very high temperatures where vaporization and nucleation processes result. Recognizing wide lube oil consumption rates, let us assume an extreme, but for an older engine not unrealistic value of oil consumption at 1 % of the fuel-consumption: Then the Zn emission can be estimated at about 1 mg/km. Moreover, Ca is emitted and all other abraded metals. Modern engines, properly maintained and rather new, emit a tenth of that value. Investigations comparing Diesel and CNG engines [31] report Zn emissions of 0.2 mg/km from Diesel and 0.4 mg/km from CNG. One DI Diesel engine study [33] meticulously tracked the metal content of lubrication oil. The results show that most of the metal oxides remain in the engine, e.g. 69 % of the Zn. The exhaust emission of Zn, depending on the operating point, was up to 0.1 mg/km. The Ca emissions were fourfold. Substantial higher emissions can be expected from small two-stroke engines. These are deployed in mopeds, motorbikes and hand held equipment such as chain saws. These engines are lubricated by adding > 2 % of lubrication oil to the fuel. The specific fuel consumption is higher, too. Thus, the specific metal emissions are at least four times those from above discussed larger 4-stroke engines. Metal-free lubrication oils were investigated [34] for mixing with two-stroke fuel. The manufacturers predict comparable performance for the non-metallic lubricants. Without legal compulsion, however, such lubrication oils will only be deployed in special situations [35]. It is noted 2-stroke emission most often occur in operators breathing zone. Many emerging and developing countries unfortunately tolerate metallic fuel additives. The resulting emissions of ash particles were recently investigated by Gidney et al. [36] on a gasoline passenger car. The fuel additives were Mn, Fe and Pb in concentrations up to 18 ppm. Very high metal-oxide exhaust emissions of up to 2×10^8/cc were measured at a size of about 10 nm. This scenario is still realistic in some countries. This could become a problem with the use of so-called fuel borne catalysts (FBC). These are metal-organics added to the fuel in very small concentrations to promote regeneration in Diesel particle filter systems (DPF). Results are reported for DPF fitted ex-factory [37] and retrofitted [38].

Figure 2 shows an example of a cerium oxide based additive in a Diesel engine [41,42]. SMPS measurements indicate a

bimodal size distribution with a marked peak at very small sizes, when the fuel additive exceeded 10 mg metal per kg fuel. The particles were collected and analyzed for their Cerium content, which proved the assumption that this peak consisted of Cerium oxide particles [42]. At additive concentrations of 5 ppm, a peak at small size ranges is not visible (see Fig.2). The metal oxide particles are probably deposited on larger soot particles (Fig. 3), whereas with increasing concentrations the peak height increases dependent on the additive dose. The soot reduction effect is also proportinal to the dose. At correct dosing levels the Ceriium oxide particles should of course be attached to the soot particles in order to be able to catalyse the soot combustion. If a separate peak appears at low particle size, which indicates a free metal oxide aerosol size class this is a clear indication of overdosing the FBC and should be avoided.

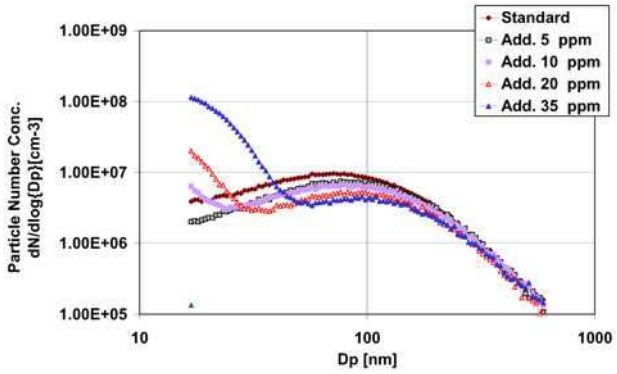

Fig.2. Particle size distribution with a FBC (cerium based additive) dosed in different concentrations [41].

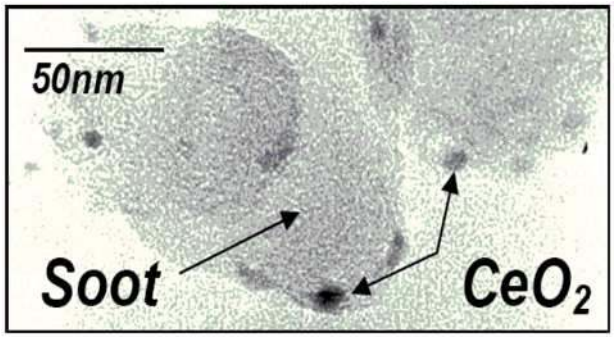

Fig.3. Cerium oxide FBC hooked on soot particles [43]

Figure 4 shows a similar phenomenon with 2-stroke scooters, according to Czerwinski [34]. When the lubricant content in the fuel is doubled (from 2 to 4 %), then a log-normal distribution is displayed with no metal oxide particles visible. If the lubrication oil content is however reduced, then the number of "soot" particles becomes so small that metal oxides appear as a separate mode at very low particle size. Once they are not longer attached to the larger soot particles, their large number becomes obvious.

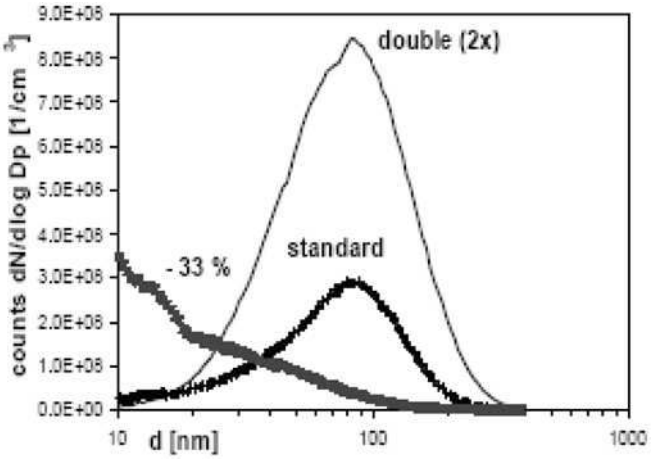

Fig.4. Particle emissions from a 2-stroke scooter engine at different lubricant ratios. Standard was 2 % of fuel. Sampling line is heated to 300 °C to suppress volatiles [34]. When large particles to attach are missing the metal oxides appear as a separate aerosol size class. Chemical investigation of these phenomena with two-stroke engines is ongoing. Metal free lubrication oils with similar performance were used and proved to be feasible.

METAL OXIDE PARTICLE EMISSIONS FROM COATINGS IN CATALYTIC CONVERTERS AND PARTICLE FILTERS

To achieve high catalytic effectiveness, a catalyst must be very finely distributed on the substrate. This enables a large number of active centers, and retards aging. If the crystalline binding weakens, then some catalyst crystallite particles might be emitted. An early 1977 investigation of this phenomenon, in a pellet catalytic converter [44] revealed an alarming result: about 0.02 mg Pt was emitted per km, representing about 2-5 g of the precious metal lost during the life of a passenger car. This catalyst type was abandoned already in the 1980s because of its high loss of precious metals and many other reasons.

A later detailed investigation of a typical modern 3-way catalytic converter [48] on ceramic monolithic substrate, showed an average Pt emission of about 100 ng/km. This is less than 1 % of the 1977 measurements but nevertheless still not a negligible amount. There is ongoing concern about the toxicity of these precious metals [73,74,75]. Higher emissions can occur for other metals, too, depending on the catalyst coating technology. For example, for US 2010 SCR, Vanadium SCR is anticipated, deployed very close to its thermal mobility threshold. Therefore, there is a compelling need to restrict and regulate such metal emissions.

NUMBER/SIZE DISTRIBUTION OF METAL OXIDE PARTICLES IN EXHAUST

The general assumption is that mechanical destruction of materials results in a particle size >1µm. However, high concentrations of metal oxide particles are also observed in the exhaust gas in the size of 10-20 nm [32,51]. This can only occur through nucleation from the gas phase [49]. That study reported the mean value of 19 nm from the log-normal distribution of iron-oxide particles originating from the intense combustion vapor phase. Lim [72] also suggests nucleation at higher engine loads. These results support the classic conclusion of Israel [30], that the metal particles are partially vaporized during combustion and nucleate from this vapor phase.

There are 2 hypotheses which might explain this phenomenon. Firstly, the so-called thermal explosion that Grigull [50] described. The heat released during abrasion is postulated to locally melt the metal. However, this hypothesis does not fully explain the vaporization, which would be needed. The second hypothesis by Israel [30] is combustion: abraded particles could be flushed into lubrication oil and then re-entrained into the combustion zone. The abraded particles may vaporize during combustion of the oil droplets, and subsequently re-nucleate. More easily explained is the formation of such small particles from the lubrication oil additives and fuel additives. These additives are metal-organic compounds; they dissociate during combustion and may then accumulate to small nm size particles.

Several studies [32] report that metal emissions in the exhaust-gas can occur in very low size classes. Hu et al published [32] metal emissions in size classes between 20 nm to 10 µm, for vanadia particles a clear bimodal distribution with relatively high concentration < 250 nm particle size was found. Lee [77] reported high number concentrations around 10 nm for Diesel and gasoline engines, both port injected and direct injected. When metallic additives are used, the particle count can increase to 10^8/cc at the size around 10 nm [36]. The same source reports on $>10^7$/cc ash particles in the size class of 10-20 nm during Diesel engine idling.

High number concentrations in small size ranges very often turn out to be condensed volatiles, generated when the exhaust cools down during dilution in the CVS-tunnel or similar processes. These usually are condensates from sulfuric products or hydrocarbons or combined and also water. If there are sufficient solid particles available, they do condense on their surfaces. If however very few particles are left in the exhaust gas downstream of an efficient particle filter, there might be sponaneous condensation generating these very small droplets. This can be very misleading if no chemical analysis is performed or solids and volatiles are not clearly separated during the evaluation. For separation solids from volatiles in the past very often thermodenuders were used, some researchers also use catalytic strippers. UN-ECE R83 (PMP) [58] came to the conclusion that a combination of diluting 1:100 and heating the exhaust gas > 300 °C to vaporize all volatiles is a very reliable method. The above method was used for the investigtions reported below. Many publications are available investigating these effects [35,57,59,80,81,82,83,84,85]

The combustion generated metal oxide particles can most likely deposit on soot particles. If there are only few soot particles, then the metal-oxide particles possibly appear as unattached aerosol size class in the exhaust gas. Since common particle counting instruments such as SMPS provide no chemical information, attached metal oxide particles cannot be distinguished from soot particles in the size distributions. Unattached metal-oxide particles however manifest as a distinct bimodal distribution. The metal-oxide particles peak occurs at about 10-20 nm, as shown in Fig.2 for fuel additives. It can be assumed that not all metal-oxide particles are to be found in this peak of unattached aerosol components. Some of the metal-oxide particles might also be included in other size classes due to deposition on larger soot particles. So far we do not know whether they will detach after entering the organism. A quantitative analysis thus requires investigating the composition of all size classes.

Respiratory air at heavy traffic locations contains in the particle fraction below 180 nm (PM 0.18) according to Sioutas, mainly the following metal constituents [79]:

Ca: 2.77 %

Al: 1.24 %

Fe: 0.92 %

Cu: 0.12 %

Zn: 0.20 %

In total about 5 % of the overall mass of the sample in the size range < 180 nm consisted of metals. This confirms the determined 3% in the exhaust of HDV [32]. Cho [78] also reports on high concentration of Zn, Ca, Fe, Cu and Al in ambient air close to an urban highways in coarse (2.5 - 10 µm), fine (0.1 - 2.5 µm) and ultrafine (< 0.1 µm) size classes.

Summarizing prior publications: Diesel engines emit metal-oxide particles from 0.1 mg/km (LDV) to 1mg/km (HDV). SI engines might emit the double [31]. Some of these particles are emitted in the mobility size of 10-30 nm, i.e. in the deposition-maximum of the alveoli. The metal-oxide particles are mostly insoluble and therefore prevalent persistent. Transition metal-oxides are chemically very active

at their surface and this surface is specifically large due to the small particle size. Thus, these fulfill all criteria of a very toxic air pollutant. Are these metal oxide particles the actual toxic substance of engine emitted solid particles? This is possible, because biological activity and toxicity strongly depends on the nanosize particle type and its chemical composition [52]. Therefore, this aspect must be investigated to develop appropriate control technology for capture and elimination of this size specific fraction in the exhaust.

SIZE-CLASSIFIED METAL ANALYSIS FOR EMISSIONS OF DPF SYSTEMS

The specified methods in the VERT suitability test procedure are briefly described below. Additional results are presented in the following, too. Best available particle filter technologies (BAT-DPF) are fully developed, available on the market and proven to very efficiently remove the solid nanoparticle fraction from diesel engine exhaust. However more work is indicated for actual SI engine applications [59,61,63].

The VERT tests [56] were developed 1993-2000 and since then constantly improved. From 1998 onwards, the tests are routinely used for suitability testing and approval of particle filters in Switzerland and other countries. Moreover, the VERT procedures are also used for workplace certification in Germany and Austria. Recently, the VERT tests were codified in the Swiss standard SNR 277205 [57]. The VERT instrumentation and procedures are the forerunner of the UN-ECE R83 (PMP) procedure. PMP is the basis for new European emission legislation [58]. Beside filter effectiveness, VERT also tests many other application criteria [59]. Those include secondary emissions [56] and the size specific emissions of metal oxide particles [61].

The ISO 8178/4 driving cycle (C1 Fig.Fig.5) is used to determine secondary emissions and metal oxide emissions. The cycle is driven twice in the legally specified sequence. The total operating time is 200 minutes. This long time is necessary to collect sufficient material for the trace analysis. There is no pause between the individual operating points. Instead, the transition is regarded as realistic transient feature in the analysis. The temperatures are in a band, which facilitates the formation of secondary emissions, e.g. the de-novo synthesis of dioxins [22].

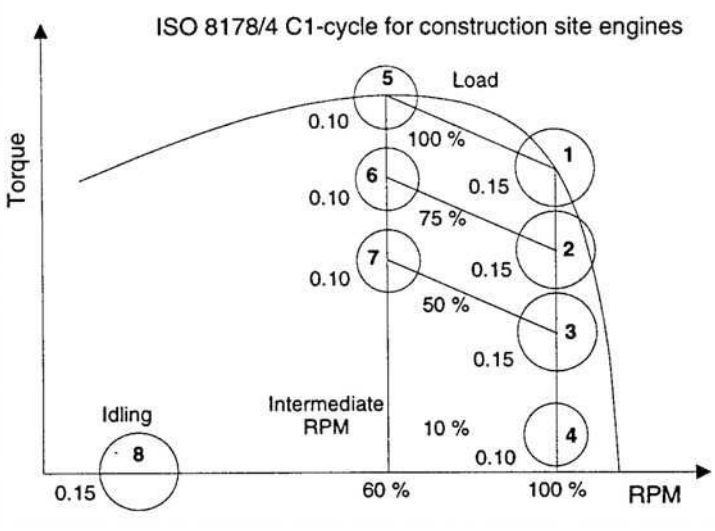

Fig.5. ISO 8178/4 C1 driving cycle used for VERT suitability test for particle filter systems to assess potential of the formation of secondary organic and metal oxide emissions

At high loads (1-2-5-6), oxygen supported regeneration of the particle filter occurs. Thus, all pertinent phenomena are captured, too. It must however be emphasized that due to this repeated regeneration phases, the filter remains very clean throughout this test. Thus this procedure represents a worst case scenario for all filtration phenomena as intended by VERT.

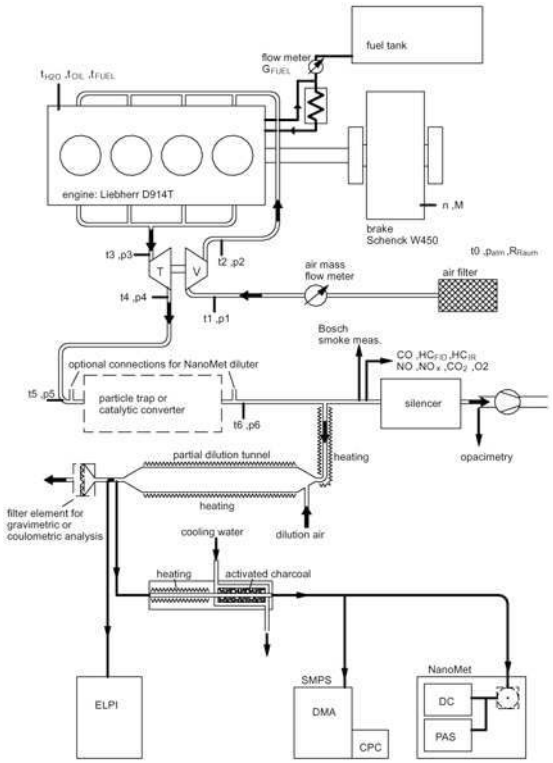

Fig. 6. Test setup

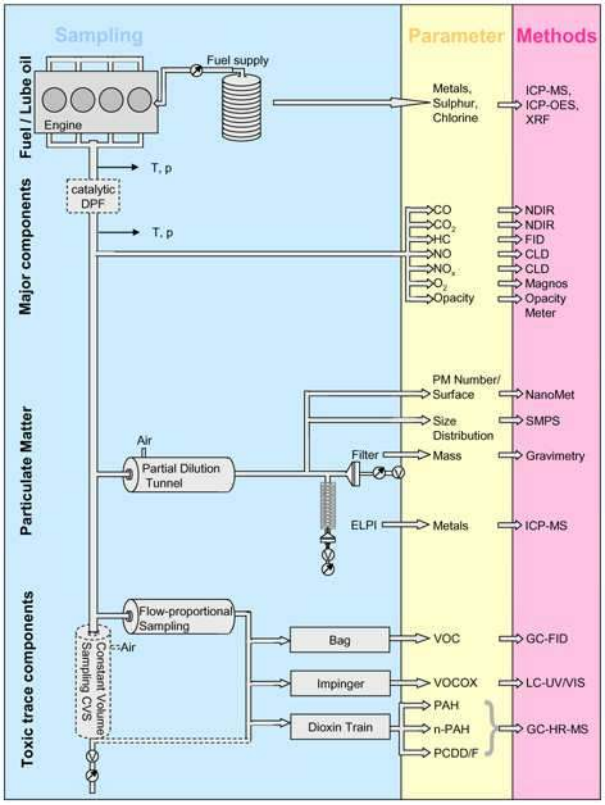

Fig.7. Sampling and instrumentation schematic

Fig. 6 is a schematic of the VERT test rig. It shows the setup for both the gas measurement and the granulometry. The particle sampling for the size specific metal analysis uses an Electrical Low Pressure Impactor ELPI for size-dependent particle collection.

Flow proportional undiluted sampling, during the entire test time, is used to determine trace compounds, VOC and PAH (Fig.7). Partial flow dilution, using an AVL Smart-Sampler is used for granulometry, gravimetry and for the size-specific metal analysis following ELPI size fractioning. Standard gases are measured direct as usual, NO_2 with heated sampling line and dryer membrane.

For size-fractionated metal analysis, the exhaust-gas is diluted about 1:10. Then the ELPI impactor partitions it into 13 size classes in the range from <30 nm to 10 µm. The analysis, of the collected aerosols on the impactor films, is performed according to a microwave assisted acid digestion procedure with subsequent ICP-MS analysis, as described below.

METAL ANALYSIS METHODOLOGY

The ultra-trace determination of metals requires a strict optimization of the entire sampling procedure, sample preparation and analysis. Sampling mistakes can yield misleading results [61].

Sampling using ELPI

For sampling, the ELPI was equipped with pure polycarbonate collector foils for each size stage. A back-up filter collects the size fraction below 30 nm. All filter materials were validated prior to testing for low contamination levels [62].

Sample preparation and analysis

All samples were digested with acid mixtures in a microwave oven. The vessels used for the digestion should be carefully pre-cleaned and validated before use to achieve best detection limits.

All cleaning digestions must be verified using highly sensitive analytical techniques like ICP-MS (inductively coupled plasma mass spectrometry) to ensure that the vessel background levels are low enough for such ultra-trace analysis. Only ultra-clean vessels should be used.

Depending on the filter material and the pertinent target elements, sampling filters were digested with the following acid mixtures in a microwave oven:

- Nitric acid HNO_3
- A mixture of nitric acid HNO_3 and hydrogen peroxide H_2O_2

• A mixture of nitric acid, hydrochloric acid HCl and hydrogen peroxide H_2O_2

Further details on the digestion procedure, e.g. the exact temperature-time programs for the microwave oven, can be found in [62].

The resulting solutions were analyzed using plasma mass spectrometry ICP-MS. Depending on the analyte elements, either a quadruple ICP-MS (ELAN 6000, Perkin Elmer/ Sciex) or a high resolution ICP-MS (ELEMENT 2, Thermo Finnigan) were used.

Reliable results can only be achieved if the detection limit of the entire procedure, including sampling, sample preparation and analysis are determined. Therefore, blanks of fresh filter material and field-blanks (processed similarly to field sampling filters) need to be sampled, digested and determined.

Contamination risk and memory effects are not negligible especially for ubiquitous metals like Fe. Usually the metal determination is more limited by the sampling procedure and sampling preparation than by detection limits of the analytical method.

TEST ENGINES, FUEL AND LUBRICATION OIL

Table 1. Test engines

Manufacturer:	LIEBHERR	
Type:	D934S	D914T
Cylinder volume:	6.36 dm^3	6.11 dm^3
Rated speed:	1800 RPM	2000 RPM
Rated power:	105 kW	110 kW
Model:	4 cylinder in-line	
Combustion process:	Direct injection	
Injection pump:	Bosch unit pump	
Supercharging:	TC / IC	TC
Emission control:	EGR	-
Designed:	2005	1995
Lube oil consumption	0.1 % of fuel cons.	
Lubrication oil consumption can be higher for the new engine (first 100 operation hours) and also during extended idling.		

Table 2. Fuel: SN 181160-1:2005 Class D

Density (at 40°C)	0.820 - 0.845 g/ml
Viscosity (at 20°C)	2.0 – 3.2 mm^2/s
Flame point: min	62°C
Cloud point :max	- 10°C
Filtering limit	CFPP max. - 20°C
Coke residue	max. 0.02 g/100g
Ash	Traces
Sulfur	max. 0.001 g/100g
Cetane index	min. 52 – 54
Boiling analysis	min. 98 vol %
Calorific value (lower)	min. 42.5 MJ/kg

Table 3. Lubricant: 15W/40

Viscosity kin 40°C	-	mm^2/s
Viscosity kin 100°C	13.98	mm^2/s
Viscosity index	-	(--)
Density 20°C	-	kg/m^3
Pour point	- 25	°C
Flame point	-	°C
TBN	8.4	mg KOH/g
Sulfur ashes	10 770	mg/kg
Sulfur	3 360	mg/kg
Mg	< 10	mg/kg
Zn	1 200	mg/kg
Ca	2 630	mg/kg
P	1 110	mg/kg

RESULTS OF THE SIZE SPECIFIC METAL ANALYSIS

Two systems were investigated:

Case A. Engine Liebherr 924 with a precious metal coated SiC wall flow particle filter system (Pt,Pd)

Case B. Engine Liebherr 914 with a base metal coated Cordiererite wall flow particle filter system, which was regenerated with the aid of a fuel borne catalyst (Fe + Sr) overdosed at 40 ppm metal sum.

In both cases first the engine without filter was investigated as a baseline. In case A engine with filter followed. In case B there is one additional combination: engine without filter but with FBC and finally the particle filter was used together with FBC of course.

SMPS particle size distributions.

The PMP sampling procedure was used before size classification and particle counting [57,58]. The PMP sampling comprises 1:100 dilution with particle free air, then heating the exhaust gas to 300°C to assure, that all volatile particles (“droplets”) are vaporized and only solid particles measured. This analysis was performed at each operating point of the ISO 8178 stationary test cycle and hence 8 SMPS spectra are shown 10 nm - 400 nm for each test case

representing the 8 operation points acc. to Fig. 5. Total sampling time was 200 min, distributed acc. to the weighing factors. At least 3 scans are done for each spectrum. Point 8 represents low idle.

Fig. 8a and 8b represent results from system A. Its ceramic wall-flow filter substrate is coated with Pt and Rh to accelerate regeneration from deposited soot. Hence, these 2 elements were analysed to investigate the reliable binding of the catalytic site crystallites. In addition the engine wear metals Fe and Ni and the lubrication oil package metals Zn and Ca were analyzed.

Remarkably in Fig 8a, at 7 of the 8 operating points, the engine out particle size distribution is mono-modal, independent of RPM and load. Only the idling point has a different pattern. Meanwhile, more than 20 particle filter systems were tested according to this testing procedure. All show the same pattern: at the idling point, there is excess air and thus relatively low concentration of the soot in the exhaust gas. The typical soot peak around 100 nm is almost imperceptible at this scale. However, a peak occurs for very small particles in the size range 10 - 20 nm, which cannot be explained by volatiles since PMP sampling treatment with 300°C heating was applied. These must be solid particles, which are not soot particles, thus they can only be ash particles. The results can be explained by the following hypothesis: these small particles originate from lubrication oil, since the lubrication oil consumption is very high at idle. This is caused by the fact that the engine blow-by gas flow from cylinder to oil sump, which usually pushes back the lubrication film, is very weak at idle. Thus more lubrication oil and thus more metals intrude into the combustion and consequently into the emission spectrum. At idle, these very fine metal-oxide particles most likely find few soot particles to attach on. Therefore, the metal-oxide particles remain unattached and are visible as a separate peak. Metal-oxide particles are also prevalent at other operating points, but probably deposited on larger soot particles. These metal-oxide particles doubtlessly remain undetected here for the operation points 1 - 7 until analyzed by size fractioned chemistry (see table 4 and 5)

Figure 8b presents the data downstream of the particle filter. The entire spectrum is suppressed by more than 2 orders of magnitude, whereas the effectiveness seems to be a little bit better at lower loads - which might be an space velocity effect. Overall filtration performance integrating all particle size classes and all operation points turned out to be 99.35 %. Surprisingly, the peak at the idle point almost completely disappears, which is explained by the fact that diffusion dominated filters like this one intercept these very small particles even more efficiently than larger nanoparticles.

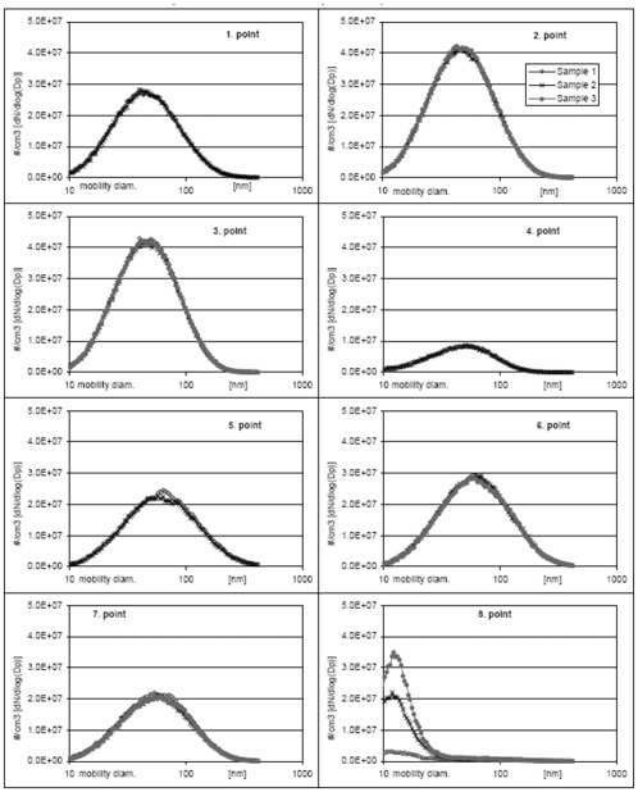

Fig. 8a. Case A: Baseline, particle size distribution of the Liebherr 924 engine without DPF. SMPS measurements at 8 operation points acc. to Fig.5. Point 8 is idling at 800 RPM..

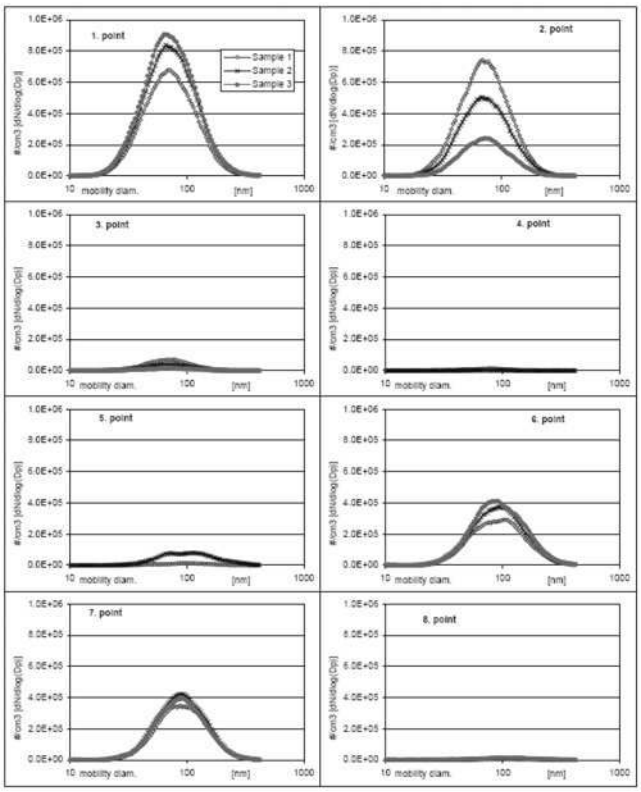

Fig. 8b. Case A: particle size distribution of the Liebherr 924 engine equipped with a coated DPF. SMPS measurements at 8 operation points, downstream of the particle filter system.

Figure 9 illustrates the filtration characteristic using the parameter penetration, which is defined as follows penetration = 1- filtration effectiveness; This parameter is calculated with the data of Fig. 8b divided by the data of Fig 8a.

These filtration characteristics permit interesting interpretations. Effective filtration occurs both in the diffusion range and also in the impaction range, but better in the diffusion range. Whereas filtration is 99.99 % at nearly all operation points for particles as small as 20-30 nm is "only" 99% for the largest soot particles of 300 nm mobility diameter.

This shaping of the filtration characteristics depends on face velocity of the gas through the walls, pore size and wall thickness. This ceramic wall flow filter did in fact have a mean pore size of 19 µm, and with 190 cpsi a low face velocity which favors the diffusion mechanism. Basically this is a good property from health perspectives. As a result of this the very small metal oxide particles are no longer visible in the spectra downstream of the filter. The opposite, favoring impaction filtration, should not happen - it would result in low particulate mass, but high particle number downstream filter.

The 3 following diagrams Fig.10a, b, c show Case B with an older engine, Liebherr 914, without and with a base metal coated Cordierite filter. This filter system uses a Fe + Sr containing metal-organic fuel additive for regeneration, which is overdosed at 40 ppm metal sum as required by VERT for test purposes.

Basically these 2 engines are not to different designs, but 2 generations. Both were exclusively used for research purpose, so overall operation time is relatively short and proper maintenance is guaranteed. During these tests both were in excellent condition with respect to wear and lubrication oils consumtion.

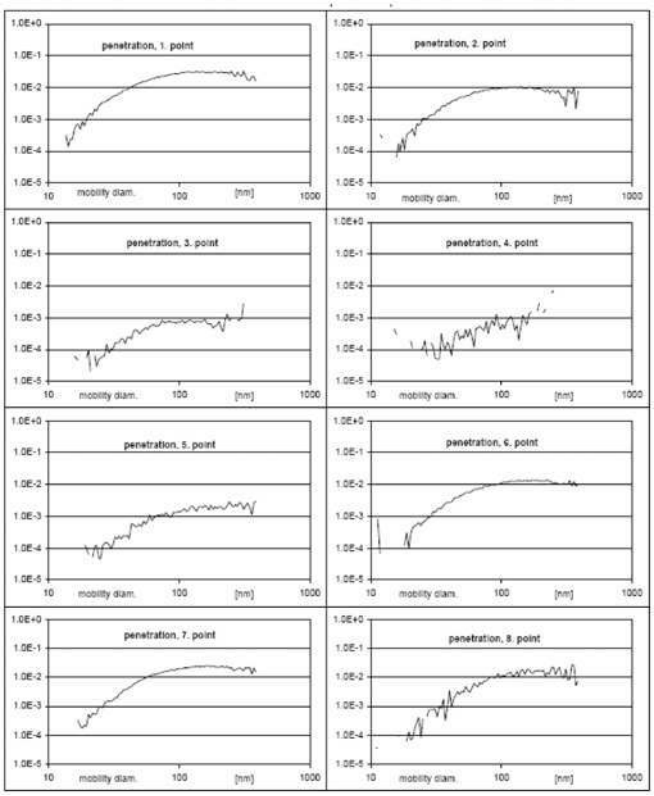

Fig.9. Case A: Penetration at the 8 operating points of the coated filter, calculated from Fig.8a ***and*** 8b

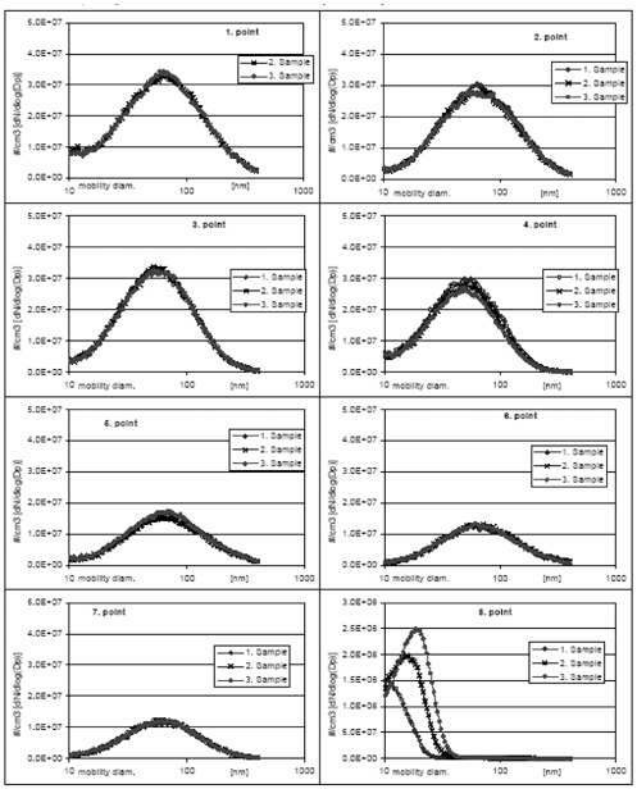

Fig.10a. Case B: baseline of the engine Liebherr 914 without DPF and without FBC

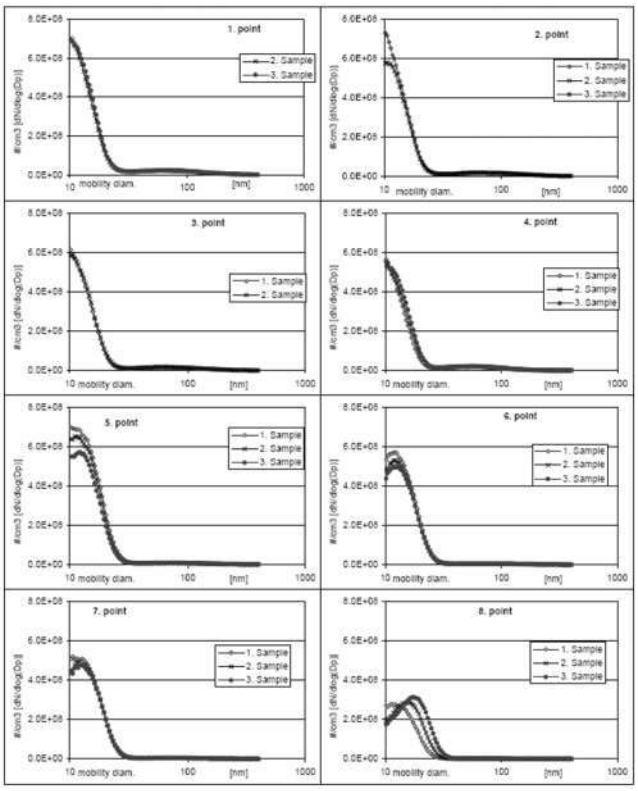

Fig.10b. Case B Liebherr 914 engine without DPF and with FBC, at constant overdose rate of 40 ppm Fe + Sr − metal.

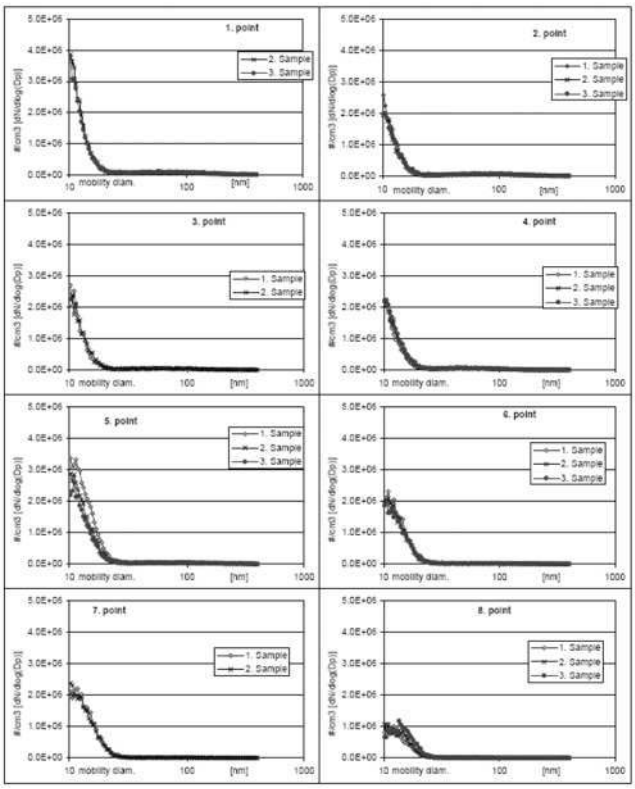

Fig.10c. Case B: Liebherr 914 engine, with base metal coated DPF, operated with 40 ppm FBC overdose. Measured downstream DPF.

The distribution, Fig.10a, is again mono-modal and log-normal at the operation points 1 - 7. But at operation point 8, engine low idle, just as discussed above with case A, a very high particle number concentration peak is observed in the range of again 10 -20 nm, showing a bi-modal size representation, whereas the soot peak, being much lower is suppressed due to the selected linear scale. Most likely these are again ash particles originating from the lubrication oil.

Figure 10b shows the same configuration, still without DPF but with the fuel additive. The metals contained in the metal-organic additive are oxidized during combustion. The normally deployed FBC concentration is 10-20 ppm. However the tests were performed at the higher concentration of 40 ppm in the fuel to intensify the effects. The FBC is dosed at constant concentration to the fuel. This is obviously overdosing. Although there is enough soot available to attach on, many metal oxide particles remain free in the exhaust gas and form a separate peak in this bi-modal distribution around 10-20 nm at all operation modes. At idle, despite low metal amount due to the low fuel quantity and very high dilution by air excess, the particle number concentration in the size range 10 -20 nm is on average somewhat higher than in the previous case A. Most likely these are partially the additive particles plus ash particles from the lubrication oil.

In Figure 10c, the engine is equipped with a very efficient particle filter and operated at the same dosing rate of 40 ppm. Shown is the size distribution after the particle filter. The investigated filter system diminishes soot particle emissions by about 2-3 orders of magnitude. The high peak of additive dosage, is reduced by more than 3 orders of magnitude, but remains still visible in the size distribution.

Figure 11a and 11b plot the penetration characteristics of the DPF with the metal-organic additive at 40 ppm metal concentration. Fig.11a compares particle number downstream filter to upstream filter both with FBC- dosing. This is the true penetration characteristic. It is very balanced, penetration remains on a level of 0.004 at all particle sizes and for all operation modes, a very good filtration result. Fig. 11b compares particle number downstream filter with FBC to engine baseline without FBC. Here the additive peak is still visible except for idling in mode 8, where due to the very low space velocity diffusion is even stronger.

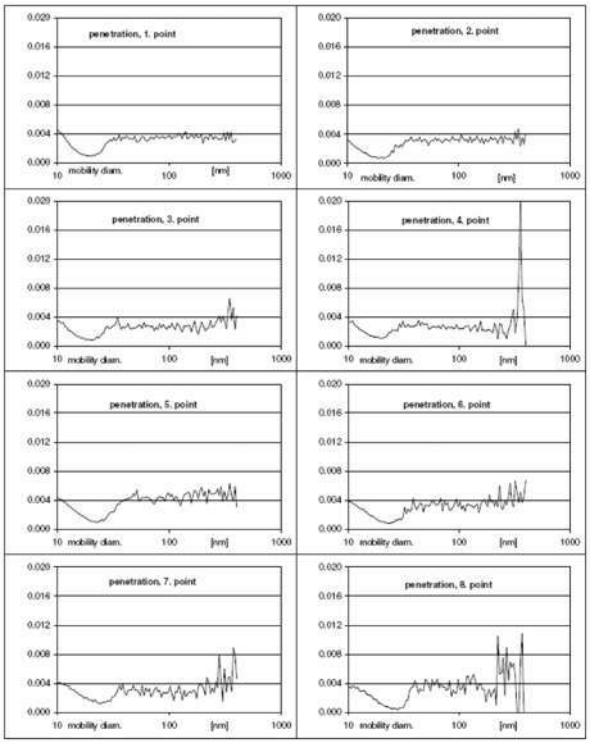

Fig.11a. Case B: Liebherr 914 engine with DPF and with FBC, comparison of PN downstream filter to upstream filter; dividing PN of Fig 10c ***/*** Fig 10b***.***

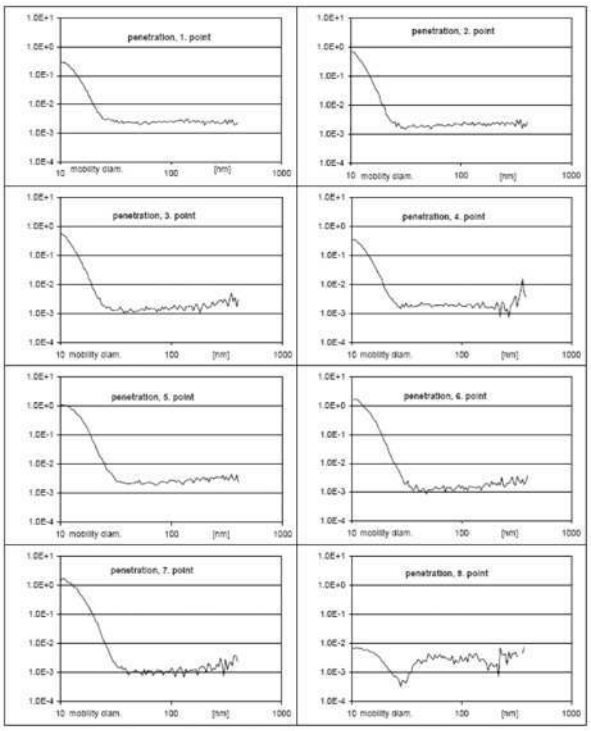

Fig.11b. Case B: Liebherr 914 engine, comparison PN downstream filter with FBC to baseline without FBC; dividing PN of Fig 10c / Fig 10a**.**

Belot *et al* [37] demonstrated that fuel additive promoted regeneration is more effective than regeneration by catalytic coatings. This despite the higher FBC reaction temperature of 320°C, compared to 240°C for NO_2 induced regeneration. Fuel borne catalysts function according to the principle of homogeneous catalysis. The catalyst is in-situ generated and directly active in the soot particles, whereas catalytic coatings function according to the principle of heterogeneous catalysis which requires a direct contact with the surface. Hence, non-removable ash deposits covering the coating can decrease regeneration efficiency over time causing longer periods of no or less thorough regeneration whereas fuel borne catalysts are always freshly dosed. FBC are generally reducible oxides such as Fe and Ce, which promote atomic rather than molecular oxygen. Diesel exhaust has plenty of oxygen available. Hence, the induced regeneration is faster, more exothermic and thoroughly advantageous for effective cleaning of the filter. Moreover, Fe and Ce additive supported regeneration is independent of the fuel's sulfur content and does not release NO_2. Therefore, fuel additives intrinsically do not age nor decline in performance with time. Moreover, variable dosage facilitates elegant adaptation to practical requirements.

However, a major disadvantage of the application of fuel borne catalysts FBC is the collection of the additive ash in the filter matrix with the risk of clogging the particle filter faster and the consequent risk of possible metal-oxide particle emissions. VERT therefore requires for all FBC systems that the filter substantially intercepts the emission of additive particles. When a Fe additive is used, the Fe emissions must be less than the raw Fe emission of the engine. Moreover other control measures are required, e.g. continuous monitoring of the system; immediate and automatic stop of additive dosing if the onboard control detects DPF malfunction.

Size dependent chemical analysis for case A with precious metal coating

During the online investigation for particle size distribution one part of the exhaust gas passed a partial flow diluter and the ELPI impactor as shown in Fig.6 and 7. After the test the deposited particulate matter, collected during 200 min. of 2 complete ISO 8178 test cycles on the 12 polycarbonate collector foils of the ELPI impactor plus the quartz backup filter for the finest fraction, was ICP-MS-analyzed, as described in the previous section. The results are summarized in Tables 4, 5 and 6. Tables 4 and 5 shows the metal emission analysis from the 200 minutes test, passing all 8 modes; Table 4 represents data without filter and Table 5 with filter. Beside of the coating metals Rh and Pt also wear metals Fe and Ni and lubrication oil metals Zn and Ca were selected for this analysis. Table 6 are results from the idle mode 8, which was run separately.

<tables 4, 5 here>

Without particle filter, Table 4, the engine Fe-emission, corrected for blanks reached 1.21 µg determined as sum of the 13 ELPI stages - which corresponds to 0.038 mg/kWh (calculation method see [63]), the Zn-emission was even higher with 1.87 µg and the Ca-emission was much higher. All analysed metals together come to an emission of 1.5 mg/kWh, which seems quite high and supports the message of this paper to scrutinize metal emissions of engines and find technical solutions to eliminate them.

With the installed particle filter, Table 5, the Fe-emission was diminished to 0.03 which is only 2.5 % of the engine out Fe-emission, a remarkable result; the Zn-emission was reduced to 11 %. The reduction effect for Ca was not so high. While the detection limits are very low, the contamination of the deposition films and the backup filter with these metals is relatively high, particularly for Ca which makes the results a bit uncertain. Emission of precious metals from the filter coating could not be detected.

<table 6 here>

In Table 6 only the idle mode 8 was investigated, particulate material was sampled during 120 min of continuous idling at 800 RPM and then treated exactly as the other samples described above. The results can be directly compared when

corrected with the sampling time difference. Overall emissed mass of all metals during this idle mode are very close to the overall emissed mass during the full cycle. This is quite surprising since during the operation points 1 - 7 engine speed and engine power are much higher. More than 50 % of the metals Fe and Zn is found in the size classes < 60 nm which perfectly supports the assumption that the high peaks observed during mode 8 in Fig 8a and 10a consist of tiny metal oxide particles. The explanation is the high oil consumption during idle condition and this is not only the explanation for the lubrication oil package metals Zn and Ca but also for the wear metals Fe and Ni since those Fe- and Ni-particles, which we are finding here are not direct wear particles, but indirect wear particles, which are re-entrained with the lubrication oil into the combustion process.

Size dependent chemical analysis for case B with base metal coating and FBC Fe+Sr

<tables 7, 8 here>

Table 7 and 8 show the data for the particle filter system B operated with a fuel additive containing Fe and Sr in metal-organic form. Table 7 is for the Fe-analysis, Table 8 for the Sr.analysis. Three combinations were analysed: first with a non-doped reference fuel for the baseline raw emissions without filter; second, the raw emission with the overdosed additive but still without DPF; and finally DPF with the additive doped fuel.

Although the idle point was not analysed separately here and only the FBC elements Fe and Sr were analysed, the results are again interesting. 5.69 µm (corrected for blanks 2.45 µm) iron are emitted by the engine which translates to 0.18 mg/kWh (0.08 mg/kWh). This is high enough to explain the peak at idle observed in Fig.10a together with the emissions of Zn and Ca, which can be assumed based on the findings with system A. Practically no additized iron penetrates the filter. The emission is equal to engine out emission. This is not fully satisfying since Fe-emission should be close to zero but the result is to some unknown extent uncertain because of the contamination of the ELPI films and filter due to the ubiquity of iron in the environment. From an analytical standpoint this should be better with Strontium and indeed with the Strontium FBC the penetration 0.165 / 19.16 comes to the very low level of 0.008 and the emission of Sr-particles to the atmosphere is close to the detection limit.

The metals are not only detected in the smallest size fractions, but also in larger ELPI size classes. The initial metal-oxide particles are intrinsically not large (only 3-5 nm primary particles). Instead, small particles seem to be deposited on larger soot particles and jointly collected on the corresponding impactor stage. The ELPI method as used here is not sufficient to tell the truth about the size of the metal particles, supplemented by the SMPS size distribution the phenomena become clearer but ultimately the metal particles should be separated by burning the soot of in the aerosol phase and classify. This might be an interesting analytical proposal by whether after inhaling and penetrating into the organism the metal oxide particles are separated from soot particles or so far unknown.

THE MIGRATION PROBLEM

Particles are intercepted in the porous filter matrix through diffusion or impaction. Van der Waals forces bind the deposited particles to the pore surface. The binding is stronger for small particles. Hence, small ash particles once attached are difficult to remove. Aerodynamic effects certainly cannot remove these. Larger agglomerated ash particles are more likely to eventually escape the filter matrix.

The situation can become critical for nanosize ash particles, especially those additive particles deposited on soot particles and trapped as agglomerates inside the filter matrix. When such a filter is regenerated, i.e. the soot in the cake burns, than the metal oxide particles might suddenly become entrained in the flow and escape, unless further filtration occurs. Hence there is a risk of a certain emission of metal-oxide particles during filter regeneration. High space velocity and large pores exacerbate these metal oxide emissions due to migration. Efforts must be made to prevent it. Membrane filter technology [64] might be advantageous and more suited to reduce these effects.

It should be emphasized that this is a worst case scenario that happens with new filters only. Once an ash cake has been formed, this does probably not happen to the same extent. For SI engines, the buildup of a metal oxide filter cake will certainly take longer than for CI engines to eventually attain sustained hot-gas penetration rates. Nevertheless, efficient hot-gas filtration designs are anticipated to eliminate toxic metal-oxide emissions from all combustion engines.

CONCLUSION

Beside of soot particles, diesel engines also emit metal oxide particles, generated by wear processes as well as by nucleation during the intense combustion process. Wear processes generate particles in the µm range whereas nucleated particles can be much smaller and normally found in ultrafine nanometer range. These can be: typical wear metals like Fe, Ni, Cu; or metals originating from lubrication oil packages like Zn and Ca; or metals from fuel additives used for DPF regeneration where Fe, Pt, Ce and other is used; and all can enter the combustion process. Finally catalytic metals from emission control devices can be eroded. All of these become airborne and enter into human breathing environments. Nanosize metal oxide particles are observed to be emitted attached to soot particles and also as free particles

in the size range of 10-30 nm with concentrations as high as 10^8 particles per cc, as observed during idle conditions.

Particle emissions generated by internal combustion engines are today recognized as the most serious urban air pollutant. Technical countermeasures are required to eliminate these particles, which are more dangerous the smaller they are. The true toxic substance can be: the elemental carbon of soot; or the organic deposits on the soot particles; or the attached metal oxide particles; or the combination. The definitive cause is still unclear and requires further investigation. Much evidence points to engine emitted metal-oxide particles being those of the most health concern.

There are two practical and proven technologies available to rectify the problem:

• Firstly, deploy highly efficient particle filter systems on all combustion engines as this paper demonstrates in 2 cases with VERT-certified particle filter systems: one regenerated with the aid of a precious metal catalyst coating; the other with a base metal coating and fuel borne metal catalyst.

• Secondly, diminish the metal content of the lubrication oil, which has been investigated with small 2-stroke engines and described in earlier SAE-papers.

Since technologies are available and health concerns are mounting, further emission curtailment requires that the size dependent chemical composition of IC engine exhaust particles must be addressed by engineers, scientists, and governments. Toxic substances must be specifically identified. Hence, the metal content of the particles must be determined and legislatively limited to levels as attained by best available control technology.

REFERENCES

1. Ultrafeine (Aerosol)-Teilchen und deren Agglomerate und Aggregate, Grundsatzpapier des Deutschen Berufsgenossenschaftlichen Instituts für Arbeitssicherheit BIA, 20.5.1998. Ultrafine aerosol particles and agglomerates. Publication of the German Institute for Occupational Safety

2. Kasper M. et al., PM10-TEQ, Approach to a Health-Oriented Descriptor of Particulate Air Pollution, 11th ETH Conference on Combustion Generated Nanoparticles, August 2007.

3. Limbach K. et al: Exposure of Engineered Nanoparticles to Human Lung Epithelial Cells: Influence of Chemical Composition and Catalytic Activity on Oxidative Stress. Environ. Sci. Technol., 2007, 41 (11), pp 4158-4163.

4. Karlsson H. et al.: Size-dependent toxicity of metal oxide particles-A comparison between nano- and micrometer size, Toxicology Letters, 188 (2), 2009, 112-118.

5. Jeng HA, Swanson J.: Toxicity of metal oxide nanoparticles in mammalian cells, J Environ Sci Health A Tox Hazard Subst Environ Eng. 2006;41(12):2699-711.

6. Hinds William C., Aerosol Technology, Properties, Behavior, and Measurement of Airborne Particles, John Wiley & Sons, ISBN 0-471-08726-2, 1989.

7. Gehr P. Heyder J., Particle-Lung Interactions, Marcel Dekker, New York - Basel, 2000, ISBN: 0-8247-9891-0.

8. Daunderer M., Metallvergiftungen, Diagnostik und Therapie, Kompendium der Klinischen Toxikologie, ecomed, 1995, ISBN 3-609-63700-5. Metal toxicity, diagnostics and therapy. Compendium of clinical toxicology.

9. Oberdörster G. et al., Nanotoxicology: An Emerging Discipline Evolving from Studies of Ultrafine Particles, Enviromental Health Perspectives, volume 113, number Juli 2005.

10. Gatti M., Impact on health by nanoparticles created by high temperature explosions, 8th ETH Conference on Combustion Generated Nanoparticles, August 2004.

11. Costantini M./HEI, An Evaluation of the health risk of using a cerium-based diesel fuel additive in conjunction with a particular filter, 5th ETH Conference on Nanoparticle Measurement, July 2001.

12. Costantini M./HEI, Relation between particle metal content (with focus on iron) and biological responses, 4th ETH Conference on Nanoparticle Measurement, August 2000.

13. Uptake and Inflammatory Effects of Nanoparticles in a Human Vascular Endothelial Cell Line, HEI Synopsis of Research Report 136, 2009.

14. Gojova A. et al., Induction of Inflammation in Vascular Endothelial Cells by Metal Oxide Nanoparticles: Effect of Particle Composition, Environmental Health Perspectives, volume 115, March 2007.

15. Dick C.A.J. et al., The Role of Free Radicals in the Toxic and Inflammatory Effects of Four Different Ultrafine Particle Types, Inhalation Toxicology, International Forum for Respiratory Research, 2003, 15.1, 39-52, link: http://dx.doi.org/10.1080/08958370304454.

16. Heeb N.: Effects of low- and high-oxidation DPFs on genotoxic exhaust constituents, 13th ETH Conference on Nanoparticle Measurement, June 2009.

17. Consultation on guidelines for metals and metalloids in ambient air for the protection of human health, defra, May 2008,: www.defra.gov.uk/corporate/consult/metals-metalloids.

18. Stöger T., Particle related inflammation as results from oxidative stress caused by particle surface properties and/or bioavailability of organic compounds, 11th ETH Conference on Nanoparticle Measurement, August 2007.

19. Wichmann H.E.et al, Gesundheitliche Wirkungen von Feinstaub, ecomed 2002. ISBN 3-609-16105-1 Health impact of fine dust.

20. Wörle J.M. et al., Nanoparticle Vanadium oxide potentiated Vanadium toxicity in human lung cells; Environ.Sci.Technol. 2007, 41, 331-336.

21. Ogami, A. et al., Pathological features of different sizes of nickel oxide following intratracheal instillation in rats; Inhalation toxicology, 19.Feb.2009.

22. Heeb N. et al., A, Secondary Effects of Catalytic Diesel Particulate Filters: Copper- induced de novo Formation of PCDD/Fs, Environmental Science and Technology 2007, 41(16); 5789-5794.

23. Heeb, N. et al., A,: Secondary Ef-fects of Catalytic Diesel Particulate Filters: Conversion of PAHs versus Formation of Nitro-PAHs,; Environmental Science and Technology 2008, 42, 3773-3779.

24. Bach C.et al., Emissionsvergleich verschiedener Antriebsarten in aktuellen Personenwagen, Novatlantis Report 2007, www.novatlantis.ch.

25. Ulrich A, Heeb N.V., Emmenegger E.: Chemistry of soot combustion in catalytic diesel particulate filters, 9th. Freiburger Symposium, 24.-25.09. 2009.

26. Hannoschöck N., Kolbenringschmierung und -Verschleiss, Dissertation ETH Nr. 7635, Zürich 1984 Piston-ring lubrication and abrasion.

27. Eberle K., Linear Wear of a Two-Stroke Diesel Engine Operated at Very High Temperatures, Pressures and Reduced Cylinder Lubricant Feed Rates, ETH Zürich, CIMAG 1989.

28. Hardenberg H., Schwefelarmer Dieselkraftstoff für Stadtverkehrsfahrzeuge, Der Nahverkehr 3/87 Low-sulfur Diesel fuel for urban vehicles.

29. Hildemann L.M., Chemical Composition of Emissions from Urban Sources of Fine Organic Aerosol, Environ. Sci.Technol., Vol. 25, No. 4/1991.

30. Israël G.W. et al., Analyse der Herkunft und Zusammensetzung der Schwebestaubimmission, VDI Fortschritt-Berichte, Umwelttechnik Nr. 92.

31. Gautam M. (West Virginia University), Issues in Measurement of Particle Size Distribution from In-Use Heavy-Duty Vehicles, ETH Conference on Nanoparticle Measurement, 2002.

32. Hu S., Ayala A. et al., Metals emitted from heavy-duty diesel vehicles equipped with advanced PM and NOx emission controls, Atmospheric Environment 43 (2009).

33. Grütering U.F. et al., Bilanzierung von Motorölkomponenten bei einem PKW-Dieselmotor mit Abgasnachbehandlungssystem, 15. Aachener Kolloquium Fahrzeug- und Motorentechnik 2006 Engine oil components of a passenger car Diesel engine with exhaust after-treatment. 2006 Aachen Colloquium on Vehicle and Engine Technology.

34. Czerwinski, J., Comte, P., Reutimann, F., "Nanoparticle Emissions of a DI 2-Stroke Scooter with varying Oil- and Fuel Quality," SAE Technical Paper 2005-01-1101, 2005.

35. SN 181163 Qualitätsrechtlinie für Gerätebenzine in der Schweiz Swiss qualtiy guideline for equipment-gasoline.

36. Gidney J.T., Twigg M., Kittelson D., Effect of Organometallic Fuel on Nanoparticle Emissions from a Gasoline Passenger Car, Environmental Science & Technology, 2009.

37. Belot G., Solvat, O., Marez, P., "Passenger Car Serial Application of a Particulate Filter System on a Common Rail Direct Injection Diesel Engine," SAE Technical Paper 2000-01-0473, 2000.

38. Shafer M.M., Schauer, J., Copan, W., Peter-Hoblyn, J., Valentine, J., Sprague, B., "Investigation of Platinum and Cerium from use of a FBC," SAE Technical Paper 2006-01-1517, 2006.

39. Richards P., Kalischewski, W., "Results from a ¼ Million km Heavy Duty Truck using FBC Regenerated DPF," SAE Technical Paper 2004-01-0074, 2004.

40. Olomolehin Y.et al. Antagonistic Interaction of Antiwear Additives and Carbon Black, Tribology Letters 2009, 10.1007/s11249-009-9489-4, in press.

41. Burtscher H.et al, J. Aemsol SC;. Vol. 29, Suppl. 1. pp. S9554956, 1998.

42. Skillas, Burtscher et al., Combustion science and Technology, 154,2000,259-273.

43. Macaudiere P.et al.: Series Application of a Diesel Particulate Filter with a Ceria-based nanoparticulate fuel-borne catalyst, AFS 2003 Conference Sept 29-Oct 2, 2003.

44. Hill R.F and Mayer W.J; Radiometric Determination of Platinum and Palladium attrition from automotive catalysts. Transactions on nuclear science, 1977.

45. Colombo et al. Platinum, palladium and rhodium release from vehicle exhaust catalysts and road dust exposed to simulated lung fluids, Ecotoxicology and Environmental Safety 71 (2008) 722-730.

46. Wang J. et al: Distribution of platinum group elements in road dust in the Beijing metropolitan area, China, Journal of Environmental Sciences 19(2007) 29-34.

47. Krahenbuhl U, Fragniere C, Haldimann M: An environmental case history of platinum, CHIMIA 2006, 60 (6), 337-337.

48. Edelmetall-Emissionen, GSF-Forschungszentrum für Umwelt und Gesundheit GmbH, Projektträger "Umwelt- und Klimaforschung", Abschlusspräsentation 17./18. Oktober

1996, Hannover Precious metal emissions. GSF Research Center for Environment and Health. Final presentation.

49. Bockhorn H. et al., In-situ berührungslose Bestimmung der Grössenverteilung nanoskaliger Metallteilchen, Abschlussbericht des Forschungsvorhabens 2442, Max Buchner-Stiftung, 2004 in situ contactless determination of size distribution for metallic nanoparticles. Final Report. Project 2442, Max Buchner Foundation, 2004.

50. Grigull U., Sander H.,Wärmeleitung; Springer Berlin und New York, 1979.

51. Miller A.I., The Origin and Fate of Metals during Diesel Engine Combustion, Dissertation University of Minnesota, 2005.

52. Brunner et al. : In vitro cytotoxicity of oxide nanoparticles: comparison to Asbestos, Silica and the effect of particle solubility; EST 2006, 40, 4374-4381.

53. Wick P.et al.: The degree and kind of agglomeration affect carbon nanotube cytotoxicity; Toxicology Letters 2007, 168, 121-131.

54. Azou B.L.et al.: In vitro effects of nanoparticles on renal cells; Particle and Fibre Toxicology 2008, 5:22, 1-14.

55. Lanone et al.; Comparative toxicity of 24 manufactured nanoparticles in human alveolar epithelial and macrophage cell lines; Particle and Fibre Toxicology 2009, 6:14;

56. Heeb, N.V., Ulrich, A., Emmenegger, L., Czerwinski, J., Mayer, A., Wyser, M., "Secondary Emissions Risk Assessment of Diesel Particulate Traps for Heavy Duty Applications," SAE Technical Paper 2005-26-014, 2005.

57. Testing of Particle Filter Systems for Internal Combustion Engines, SNR 277205, Source: SNV Schweizerische Normenvereinigung, Winterthur, Schweiz, 2007.

58. Euro 5/6 für PKW: EC-Regulation No. 715/2007,

59. http://ec.europa.eu/enterprise/automotive/index_en.htm.

60. Mayer A. et al.,Qualitätsstandards und Prüfverfahren für Partikelfilter zur Nachrüstung von Nutzfahrzeugen, MTZ 01/2009 Quality standards and test procedures for particle filters to retrofit utility vehicles.

61. Mayer A., Heeb, N., Czerwinski, J., Wyser, M., "Secondary Emissions from Catalytic Active Particle Filter Systems," SAE Technical Paper 2003-01-0291, 2003.

62. Ulrich A., Wichser A., Metal analysis of Diesel vehicle emissions, 6th ETH Conference on Nanoparticle Measurement, August 2002.

63. Ulrich, A., Wichser A., Analysis of additive metals in fuel and emission aerosols of diesel vehicles with and without particle traps, Analytical and Bioanalytical Chemistry (2003) 377 : 71-81.

64. Mayer A., Ulrich, A., Czerwinski, J., Matter, U., Wyser, M., "Retention of Fuel Borne Catalyst Particles by Diesel Particle Filter Systems," SAE Technical Paper 2003-01-0287, 2003.

65. Kattouah P. et al., Materials for catalyzed and non-catalyzed diesel particulate filters; 5.International CTI-Forum, July 2008 Stuttgart.

66. Karlson H.L. et al., Copper Oxide nanoparticles are highly toxic: a comparison between metal oxide nanoparticles and carbon nanotubes. Chem Res.Toxicol. published on web 08/19/2008

67. Mooney, John.J. LLC, Wyckoff, N.J. personal communication.

68. Pfeiffer, M., Votsmeier, M., Spurk, P., Kogel, M., Lox, E., Knoth, J., "The Second Generation of Catalyzed Diesel Particulate Filter Systems for Passenger Cars - Particulate Filters with Integrated Oxidation Catalyst Function," SAE Technical Paper 2005-01-1756, 2005.

69. Miller A.L. et al., Role of Lubrication Oil in Particulate Emissions from a Hydrogen-Powered Internal Combustion Engine, Environ. Sci. Technol., 41, 19, 6828-6835, 2007, 10.1021/es070999r.

70. Richards, R., "DPF Technology for Older Vehicles and High Sulphur Fuel," SAE Technical Paper 2005-26-020. 2005.

71. Riediker M., A system to test the toxicity of brake wear particles from cars; 12th ETH conference on combustion generated nanoparticles 2008.

72. ICRP publication 66 / 1994 : human respiratory tract model. Elsevier Science Inc. Tarrytown, NY.

73. Lim et al., Composition and size distribution of metals in Diesel exhaust particulates; J.Envir.Monit. 2009,11, 1614-1621.

74. Colombo et al., Pl, Pd and Rh released from vehicle exhaust catalysts …exposed to simulating lung fluids; Ecotoxicology and Environmental Safety 71 (2008) 722.

75. Ljubomirova et al.; Investigation of the solubilization of car-emitted Pt, Pd and Rh in street dust and spiked soil samples. Environmental Analytical Chemistry, June 2008.

76. Sutherland et al.; Grain size partitioning of Pt-group elements in road deposited sediments: implications for anthropogenic flux estimates from autocatalysts; Environmental Pollution 151 (2008 503.

77. Sager, T et al: Surface area of particle administered versus mass in determining the pulmonary toxicity of ultrafine and fine carbon black: comparison to ultrafine titanium dioxide; Particle and Fibre Toxicology 2009, 6:15.

78. Lee, J. et al; Effect of biofuels on nanoparticle emissions from spark- and compression-ignited single-cylinder engiens with same exhasut displacement volume; Energy Fuels 2009, 23. 4363.

79. Cho, S-H.: Comparative toxicity of size-fractionated airborne particulate matter collected at different distances from an uban highway; Environment Health Perspectives; 117, 11, 2009.

80. Araujo J., Sioutas C.et al. Ambient particulate pollutants in the ultrafine range promote early atherosclerosis and sytemic oxidative stress; Circulation Reserach 2008 :102; 589 and personal communication C.Sioutas with respect to metal composition.

81. Kasper, M., "The Number Concentration of Non-volatile Particles - Design Study for an Instrument According to the PMP Recommendations," SAE Technical Paper 2004-01-0960, 2004.

82. Maricq, M, How are emissions of nuclei mode particles affected by emission control; HEI-conference May 2009.

83. Vogt, R., Properties of exhaust particles from modern powertrain technologies; 28 Interantionales Motorsymposium 2007.

84. Kittelson, D., Characterization of Diesel Particles in the atmosphere; CRC, Final report 1988.

85. Kittelson, D., Ultrafine Particles from Engines; Vienna University of Technology; 16.Jan.2008.

86. Maricq, M., The effects of the catalyst and fuel sulfur on PM emission - with tunnel and dynamometer measurements; Published by Ford Scientific Research Labortory.

CONTACT INFORMATION

Andreas C.R.Mayer, TTM
Fohrhölzlistrasse 14b, CH-5443 Niederrohrdorf, Switzerland
Tel. +41(56)496 6414
Fax +41(56)496 6415
ttm.a.mayer@bluewin.ch

ACRONYMS and ABBREVIATIONS

AVL
AVL GmbH, Austria www.avl.com

BC
Black Carbon

BAT
Best Available Technology

BET
Surface area measured according to BET theory defined by S. **B**runauer, P.H. **E**mmett, and E. Teller describes the physical adsorption of gas molecules on a solid surface to determine the specific surface area of a material.

CARB
California Air Resources Board

CFPP
Cold Filter Plugging Point

CNG
Compressed Natural Gas

cpsi
cells per square inch; cell density of catalytic substrates and wall flow filters

CVS
Constant Volume Sampling

DPF
Diesel Particle Filter

EGR
Exhaust Gas Recirculation

ELPI
Electrical Low Pressure Impactor (Instument DEKATI, Finland)

EUDC
European Union Driving Cycle

FBC
Fuel Borne Catalyst

HDV
Heavy Duty Vehicle

ICE
Internal Combustion Engine

ICP-MS
Inductively Coupled Plasma Mass Spectrometry

LDV
Light Duty Vehicle

nm
Nanometer = 10^{-9} m; nanus (lat) and νάννος (greek)= the dwarf

nm-fraction
in agreement with the int. SI-standard all particles in the size range of 1-999 nm

PMP
Particle Measurement Program

PN
particle number concentration

RPM
Revolutions per minute

SI
Spark Ignition Engines

SMPS
Scanning Mobility Particle Sizer (Instruments TSI, USA).

TC, EC
Total Carbon, Elemental Carbon

VERT
Project to curtail Diesel engines emissions in tunnel construction sites in Switzerland

VSET
VERT Secondary Emission Test

VOC
Volatile Organic Compounds

WHO
World Health Organization

µm
Micrometer = 10^{-6} m;

Table 4. Size dependent analysis of coating metals as well as typical wear and lubrication oil metals in the exhaust gas of the Liebherr 924 engine without DPF. Sampling during 200 min of the ISO 8178 cycle.

ELPI Stages	Size class D 50%	Fe	Ni	Zn	Ca	Rh	Pt
	[µm]	[µg/stage]	[µg/stage]	[µg/stage]	[µg/stage]	[µg/stage]	[µg/stage]
Backup stage	< 0.03	1.4	0.0119	2.04	7.3	<DL	0.00004
1	0.03	0.14	0.014	0.36	8.7	0.00002	0.00012
2	0.06	0.08	0.012	0.57	8.6	0.00001	0.00005
3	0.11	0-08	0.010	0.22	2.9	0.00001	0.00004
4	0.17	0.03	0.009	0.17	2.4	0.00001	0.00005
5	0.27	0.11	0.028	0.22	3.6	<DL	0.00002
6	0.41	0.26	0.042	0.25	4.5	<DL	0.00005
7	0.66	0.09	0.011	0.19	2.1	<DL	0.00005
8	1.02	0.08	0.011	0.17	3.0	<DL	0.00006
9	1.65	0.12	0.011	0.39	9.5	0.00001	0.00016
10	2.52	1.06	0.150	0.14	4.4	<DL	0.00004
11	4.08	0.15	0.018	0.41	11.5	0.00002	0.00004
12	6.56	0.22	0.014	0.22	5.6	0.00001	0.00003
Sum with blanks		3.82	0.349	5.37	73.1	0.00009	0.00075
corrected for backup blanks		2.81	0.329	4.25	69.3	0.00009	0.00071
corrected for all blanks		1.21	0.15	1.87	45.3	0.00009	0.00071
detection limit		0.006	0.0002	0.0006	0.019	0.000006	0.00001
film blanks avge.		0.25	0.021	0.21	2.50	0.00001	0.00001
backup blank		1.01	0.020	1.12	3.80	<DL	0.00011

Table 5. Size dependent analysis of coating metals as well as typical wear and lubrication oil metals in the exhaust gas of the Liebherr 924 engine with DPF. Sampling during 200 min of the ISO 8178 cycle

ELPI Stages	Size class D 50%	Fe	Ni	Zn	Ca	Rh	Pt
	[µm]	[µg/stage]	[µg/stage]	[µg/stage]	[µg/stage]	[µg/stage]	[µg/stage]
Backup stage	< 0.03	0.9	0.025	1.16	6.0	<DL	0.00007
1	0.03	0.02	0.006	0.19	5.7	<DL	0.00003
2	0.06	<DL	0.006	0.08	1.0	0.00001	0.00003
3	0.11	<DL	0.006	0.27	2.9	0.00001	0.00007
4	0.17	0.15	0.011	0.23	5.4	0.00001	0.00004
5	0.27	0.07	0.010	0.16	6.1	0.00001	0.00009
6	0.41	<DL	0.005	0.03	0.8	<DL	0.00005
7	0.66	<DL	0.006	0.07	2.2	0.00001	0.00007
8	1.02	0.15	0.015	0.31	10.5	0.00001	0.00014
9	1.65	0.01	0.005	0.07	2.7	0.00002	0.00011
10	2.52	0.02	0.007	0.13	5.8	0.00002	0.00015
11	4.08	0.13	0.008	0.06	3.2	0.00004	0.00019
12	6.56	0.28	0.036	0.14	3.6	0.00001	<DL
Sum with blanks		1.73	0.20	2.90	55.9	0.00015	0.0119
corrected for backup blanks		0.72	0.18	1.78	52.1	0.00015	0.0112
corrected for all blanks		0.03	0.055	0.22	25.6	0.00008	0.0112
detection limit		0.006	0.0002	0.0006	0.019	0.000006	0.00001
film blanks avge.		0.25	0.021	0.21	2.50	0.00001	0.00001
backup blanks		1.01	0.020	1.12	3.80	<DL	0.00011

Table 6. Size dependent analysis of coating metals as well as typical wear and lubrication oil metals in the exhaust gas of the Liebherr 924 engine with DPF at idle. Sampling during 120 min at 800 RPM.

ELPI Stages	Size class D 50%	Fe	Ni	Zn	Ca	Rh	Pt
	[µm]	[µg/stage]	[µg/stage]	[µg/stage]	[µg/stage]	[µg/stage]	[µg/stage]
Backup stage	< 0.03	1.5	0.030	1.36	5.7	<DL	0.00007
1	0.03	<DL	0.007	0.27	2.4	<DL	0.00008
2	0.06	<DL	0.007	0.21	2.2	<DL	0.00005
3	0.11	0.04	0.023	0.07	1.5	0.00008	0.00003
4	0.17	<DL	0.004	0.26	5.9	0.00001	0.00002
5	0.27	0.05	0.010	0.16	4.0	0.00001	0.00006
6	0.41	0.03	0.008	0.06	1.0	0.00001	0.00002
7	0.66	0.02	0.012	0.12	2.5	0.00004	0.00032
8	1.02	0.06	0.010	0.23	5.1	0.00001	<DL
9	1.65	0.08	0.009	0.19	3.4	<DL	0.00002
10	2.52	0.10	0.015	0.25	4.4	<DL	0.00003
11	4.08	0.32	0.014	0.33	5.8	0.00001	0.00001
12	6.56	0.22	0.014	0.18	2.8	<DL	<DL
Sum with blanks		2.42	0.136	3.69	46.7	0.00016	0.00071
corrected for backup blanks		1.41	0.11	2.57	42.9	0.00016	0.00064
corrected for all blanks		0.56	0.013	0.53	15.8	0.00016	0.00063
detection limit		0.006	0.0002	0.0006	0.019	0.000006	0.00001
film blanks avge.		0.25	0.021	0.21	2.50	0.00001	0.00001
backup blanks		1.01	0.020	1.12	3.80	<DL	0.00011

Table 7. Size dependent chemical analysis for Fe particles, classified by ELPI (electric low pressure impactor 13 stages) for the particle filter system B operated without and with FBC containing Fe + Sr and with DPF + FBC during 200 min. of the ISO 8178 test cycle.

ELPI Stages	Size class D 50%	Baseline w/o DPF	w/o DPF with FBC	with DPF with FBC
	[µm]	[µg/stage]	[µg/stage]	[µg/stage]
Backup	< 0.03	0.03	2.44	0.04
1	0.03	<DL	2.13	0.01
2	0.06	<DL	5.88	0.02
3	0.11	<DL	4.46	0.03
4	0.17	<DL	0.96	0.02
5	0.27	0.01	1.14	0.02
6	0.41	0.01	1.15	0.02
7	0.66	0.01	n.d.	0.01
8	1.02	0.01	0.33	0.01
9	1.65	<DL	0.40	<DL
10	2.52	<DL	0.12	<DL
11	4.08	<DL	0.11	0.01
12	6.56	<DL	0.07	<DL
Sum with blanks		0.07	19.19	0.19
corrected for backup blanks		0.045	19.16	0.165
corrected for all blanks		0.045	19.16	0.165
detection limit		0.07	0.07	0.07
film blanks avge.		<DL	<DL	<DL
Backup blanks		0.025	0.025	0.025

Table 8. Size dependent chemical analysis for Sr particles, classified by ELPI (electric low pressure impactor 13 stages) for the particle filter system B operated without and with FBC containing Fe + Sr and with DPF + FBC during 200 min. of the ISO 8178 test cycle.

ELPI Stages	Size class D 50%	Baseline w/o DPF	w/o DPF with FBC	with DPF with FBC
	[µm]	[µg/stage]	[µg/stage]	[µg/stage]
Backup	< 0.03	0.03	2.44	0.04
1	0.03	<DL	2.13	0.01
2	0.06	<DL	5.88	0.02
3	0.11	<DL	4.46	0.03
4	0.17	<DL	0.96	0.02
5	0.27	0.01	1.14	0.02
6	0.41	0.01	1.15	0.02
7	0.66	0.01	n.d.	0.01
8	1.02	0.01	0.33	0.01
9	1.65	<DL	0.40	<DL
10	2.52	<DL	0.12	<DL
11	4.08	<DL	0.11	0.01
12	6.56	<DL	0.07	<DL
Sum with blanks		0.07	19.19	0.19
corrected for backup blanks		0.045	19.16	0.165
corrected for all blanks		0.045	19.16	0.165
detection limit		0.07	0.07	0.07
film blanks avge.		<DL	<DL	<DL
Backup blanks		0.025	0.025	0.025

The Engineering Meetings Board has approved this paper for publication. It has successfully completed SAE's peer review process under the supervision of the session organizer. This process requires a minimum of three (3) reviews by industry experts.

ISSN 0148-7191

doi:10.4271/2010-01-0792

SAE Customer Service:
Tel: 877-606-7323 (inside USA and Canada)
Tel: 724-776-4970 (outside USA)
Fax: 724-776-0790
Email: CustomerService@sae.org
SAE Web Address: http://www.sae.org
Printed in USA